Proceedings of the 20th International Conference on Soil Mechanics and Geotechnical Engineering– Rahman and Jaksa (Eds)

One-dimensional swelling deformation of compacted bentonite without stress history after saturation

Déformation par gonflement unidimensionnel de la bentonite compactée sans historique de contrainte après saturation

Yasutaka Watanabe
Civil Engineering Laboratory, Central Research Institute of Electric Power Industry, Japan, yasutaka@criepi.denken.or.jp

ABSTRACT: The elastoplastic behavior of compacted bentonite has been widely studied. However, it is difficult to determine its swelling index owing to the presence of nonlinearity on the *e*-log*p*' plane. This study performed a one-dimensional consolidation-swelling test using a compacted Na-bentonite, and the swelling deformation test using that without a consolidation history after saturation. Under a constant volume condition, the equilibrium swelling pressure could meet the normal consolidation line. At the beginning of unloading, the lateral pressure was almost half of the vertical pressure. As unloading proceeded, the relation between the lateral and vertical pressures was reversed. In the case of unloading without consolidation, the stress path was approximately along the normal consolidation line, although the unloading curve showed a slight nonlinearity. The plastic swelling deformation, which satisfies the Mohr–Coulomb yield criterion, presumably occurred with the occurrence of a large volume change by one-dimensional swelling. Upon unloading, a larger deformation caused the change in effective stress anisotropy; the effective stress in axial direction decreased, whereas in radial direction increased, which related to the nonlinearity of the swelling line.

RÉSUMÉ : Le comportement élastoplastique de la bentonite compactée a été largement étudié. Cependant, il est difficile de déterminer son indice de gonflement en raison de la présence de non-linéarité sur le plan *e*-log*p*'. Cette étude a réalisé un test unidimensionnel de consolidation-gonflement en utilisant une bentonite Na compactée, et le test de déformation de gonflement en utilisant celle-ci sans historique de consolidation après saturation. Dans des conditions de volume constant, la pression de gonflement à l'équilibre pourrait atteindre la ligne de consolidation normale. Au début du déchargement, la pression latérale était presque la moitié de la pression verticale. Au fur et à mesure du déchargement, la relation entre les pressions latérales et verticales s'est inversée. Dans le cas d'un déchargement sans consolidation, la trajectoire de la contrainte suivait approximativement la ligne de consolidation normale, bien que la courbe de déchargement ait montré une légère non-linéarité. La déformation plastique de gonflement, qui satisfait au critère de rendement de Mohr–Coulomb, s'est probablement produite avec l'apparition d'un grand changement de volume par gonflement unidimensionnel. Lors du déchargement, une déformation plus importante a provoqué la modification de l'anisotropie de la contrainte effective ; la contrainte effective en direction axiale a diminué, alors qu'en direction radiale elle a augmenté, ce qui est lié à la non-linéarité de la ligne de gonflement.

KEYWORDS: bentonite, swelling, consolidation, swelling index, anisotropy.

1 INTRODUCTION

Compacted bentonite is used in radioactive waste disposal to delay nuclide migration (Sellin and Olivier 2012, Chapman and Hooper 2012) owing to its low permeability. The self-sealing or self-healing ability of bentonite is required to maintain a low permeability because the gaps created by the placement of bentonite blocks during construction, erosion, cracking, and creep deformation of rocks need to be filled by swelling and deformation.

For the gap created at construction, namely technological voids, swelling is important during the process of unsaturated to saturated state. Numerous laboratory tests simulating this saturation progress have been performed under constant confinement conditions (Komine and Ogata 1999, Tanaka and Nakamura 2005). In addition, the swelling deformation of the specimens containing technological voids as well as the interaction between the swollen soil and test apparatus wall through pressure evolution (Wang et al. 2013, Zhang and Kröhn 2019, Komine 2019, Watanabe and Yokoyama 2021) have been investigated.

Conversely, because erosion and creep deformation presumably occur over a long period, the swelling deformation after saturation and self-healing is significant for the performance of an engineered barrier. Elastoplastic models are frequently applied to evaluate mechanical behavior of bentonite in radioactive waste disposal (Guimarães et al. 2013, Takayama et al. 2017), and the relationship between the void ratio and effective stress is of fundamental interpretation. According to the one-dimensional consolidation-swelling test (Chen et al. 2017, Guerra et al. 2019), upon unloading, the swelling line becomes nonlinear on the void ratio-consolidation pressure plane and the line seems to approach the normal consolidation line (Figure1). For this phenomenon, previous studies have shown interpretations based on elastoplastic mechanics, for instance, (Sahara et al. 2008) focused on the over-consolidation ratio and (Kyokawa et al. 2020) on the osmotic swelling effect. The

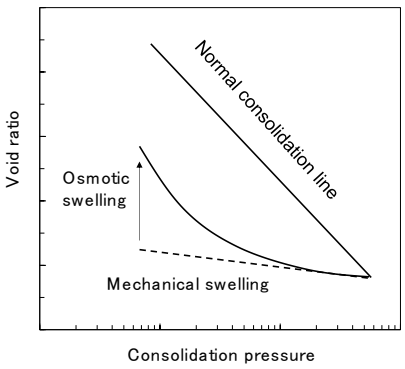

Figure 1. Features of swelling line in of expansive clays.

overconsolidation ratio is important when considering the stress history. The osmotic pressure is also necessary to examine the swelling of bentonite because it is affected by pore water chemistry. However, a unified interpretation of swelling behavior on the state plane has not yet been established, and it is still difficult to determine the swelling index.

Conventional consolidation tests include unloading after the consolidation pressure is applied to soils. Therefore, an elastic volume change, i.e., mechanical swelling, which can also be observed in non-expansive clays, is likely to occur, and it is difficult to separate it into the osmotic swelling of the compacted bentonite. For the one-dimensional consolidation, the unequal effective stress between the loading direction and that of orthogonal to loading also makes it difficult to understand the volumetric change upon unloading. Therefore, this study investigates one-dimensional swelling deformation without a consolidation history after saturation. Herein, the swelling deformation was compared with the consolidation test results. By measuring the lateral pressure during the consolidation, the relationship between the effective stresses in the vertical and horizontal directions was investigated. Furthermore, the reason why the swelling line assumes non linearity was discussed based on the relationship between the consolidation and swelling pressures.

2 MATERIAL AND METHODS

The sample used in this study included Na-bentonite (Kunigel-V1, Kunimine Industries Co., Ltd.). The particle density of the soil was 2.74 Mg/m^3, and the amount of methylene blue adsorbed was 72 mmol/100g (Tanaka and Watanabe 2019). The montmorillonite content was estimated to be 51.4%, assuming that the amount of methylene blue adsorbed on the pure montmorillonite was 140 mmol/100g (Watanabe and Yokoyama 2020).

A cylindrical specimen, 60 mm in diameter and 20 mm in height, was used for the one-dimensional consolidation and swelling deformation tests. Vertical pressure was applied to the specimen and controlled by the motorized actuator. To prevent unnecessary vertical displacement caused by the back rush of motors during stepped loading and unloading, a loading system, combining ball screws and harmonic drive motors, was employed. This system supported both strain and pressure control. The test ring involved a strain gauge inside, and the measured strain caused by the internal pressure converted to the lateral pressure, assuming that the strain occurred uniformly.

The molding water content ranged from 7% to 10%. The specimen was directly compacted into the test ring to achieve a target dry density of 1.54 to 1.58 Mg/m^3, and then the apparatus was assembled. Setting the constrained condition, deionized water was supplied from the bottom side of the specimen, and then the vertical and lateral pressures were measured. The steady value of the vertical stress at the fully water supply was defined as the equilibrium swelling pressure.

After the steady state, shifting to the pressure controlled, the vertical stress almost equal to the equilibrium swelling pressure was applied. The vertical pressure was applied step by step, checking the end of the consolidation at each pressure stage using the 3 t method. The maximum consolidation pressure was 8 MPa. In the consolidation test, the consolidation was followed by unloading of up to 0.5 MPa. Upon unloading, the swelling deformation at each pressure stage took a long period (90 days at maximum) to converge in order to obtain the vertical strain under drained conditions. Reloading was performed at 8 MPa after the unloading process. For the specimen without consolidation history after saturation, unloading was immediately performed after obtaining the equilibrium swelling pressure.

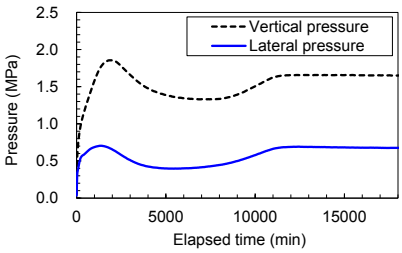

Figure 2. Vertical and lateral pressures in wetting process.

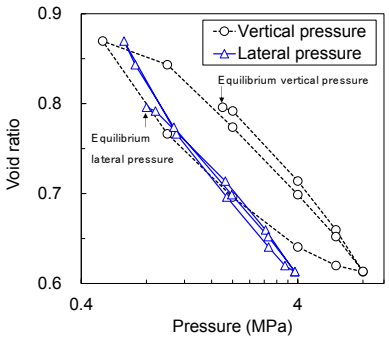

Figure 3. Relationship between the void ratio and pressures in vertical and lateral directions in the consolidation-swelling test (loading-unloading-reloading process).

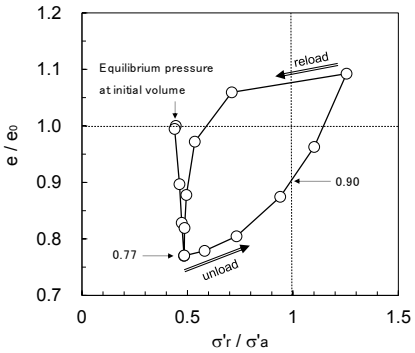

Figure 4. Ratio of effective stress in radial to axial directions (σ'_r/σ'_a) in the consolidation-unloading process.

3 EXPERIMENTAL RESULTS

3.1 *Relationship between the vertical and lateral pressures in one-dimensional consolidation-swelling deformation*

The vertical and lateral pressures during the wetting process are shown in Figure 2. Both pressures increased after water supply, and they converged to constant values. The equilibrium values of vertical and lateral pressures were 1.65 MPa and 0.68 MPa, respectively. The equilibrium vertical pressure was 2.4 times higher than that of lateral pressure.

The relationship between the void ratio and pressures in vertical and lateral directions during loading-unloading-reloading process is shown in Figure 3. Normal consolidation lines were obtained in loading and reloading paths, and the compression index ranged from 0.27 to 0.30. The equilibrium vertical pressure at the initial void ratio is located close to the normal consolidation line. The consolidation yield stress was assumed to be approximately 2 MPa.

Upon unloading, the stress path gradually approached the normal consolidation line along with a decrease in the pressure in the vertical direction. The slope between each stress point was initially 0.06 when unloading 8 MPa to 6 MPa, and finally 0.35 when unloading 1 MPa to 0.5 MPa, which was larger than that of the normal consolidation line. For the lateral pressure, there was no significant difference in the stress path between the loading and unloading processes. The slope of the linear section in the loading process ranged from 0.29 to 0.32, while the slope in the unloading process was approximately 0.33.

Note that the relationship between large and small vertical and lateral pressures has been reversed along unloading at a void ratio of approximately 0.7. Figure 4 shows the ratio of the effective stress in the radial to axial directions during the consolidation-unloading process. The effective stresses in the axial and radial directions are denoted by σ'_a and σ'_r, respectively. The ratio, σ'_r/σ'_a, was approximately 0.5 in the loading process, which corresponded to normal consolidation, and gradually increased with the increase in void ratio after unloading. When the void ratio normalized by the initial void ratio e/e_0, which was approximately over 0.90, σ'_r/σ'_a became greater than 1, i.e. $\sigma'_r \geqq \sigma'_a$. Therefore, under the one-dimensional and drained conditions, the effective stress in the axial direction was higher than that in the radial direction immediately after unloading, and the effective stress in the radial direction exceeded that in the axial direction along the swelling deformation. In addition, the effective stress in the axial direction increased immediately during the reloading process. In the reloading process, the effective stress in the radial direction was almost half of that in the axial direction in the range of normal consolidation.

3.2 *Unloading behavior of compacted bentonite without consolidation history after saturation*

The relationship between the void ratio and vertical pressure of the specimen without a consolidation history after obtaining the equilibrium swelling pressure is shown in Figure 5. The line having the slope $\Delta e/\Delta p' = 0.27$ through the initial void ratio, Δe, and the equilibrium swelling pressure, $\Delta p'$, was also described in Figure 5(a), based on the consolidation test result and the compression index. The void ratio increased because of swelling deformation owing to unloading. The stress path was approximately along the line with a slope of 0.27. Strictly, the plots upon unloading slightly diverged from the line, but the nonlinearity of the swelling line was small compared to that explained in section 3.1.

The change in void ratio upon unloading was compared with the consolidation test results in Figure 5(b). Although the initial void ratio was different, the void ratio of the specimen without a consolidation history increased with a slope close to the compression index without merging with the swelling line observed in the specimen after consolidation. As aforementioned, the swelling line after the consolidation showed a gradual increase in slope. Thereafter, the difference in void ratio at the same stress stage between the two cases became smaller along unloading.

4 DISCUSSION ON INFLUENCE OF STRESS HISTORY TO NONLINEARITY OF SWELLING LINE

The laboratory test presented the swelling deformation upon unloading of the compacted bentonite without a consolidation history, i.e. the weak nonlinearity of the swelling line and the stress path approximately along the normal consolidation line. Furthermore, the relationship between large and small vertical and lateral pressures was reversed along unloading. For the bentonite, especially the one containing a larger fraction of Na-montmorillonite, the interlaminar distance can be largely

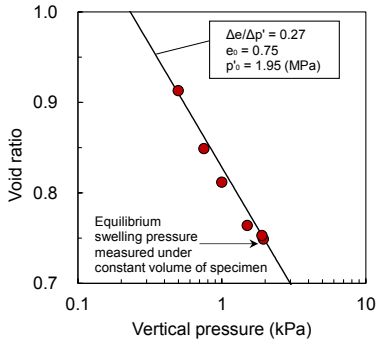

(a) Change in void ratio upon unloading.

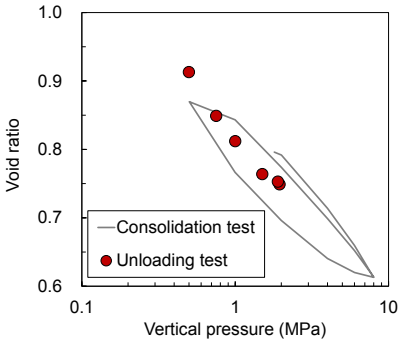

(b) Comparison with consolidation test results.

Figure 5. Behavior upon unloading of compacted bentonite without consolidation history after saturation.

expanded owing to osmotic swelling. Attractive forces, such as van der Waals forces, and the interactive physical effect of soil particles act as the constrained stress; thus, the expansion of the interlayer distance can be limited. Simply, it can be interpreted that the swelling deformation stops at balancing the swelling pressure and the external constrained pressure.

A previous study demonstrated that for swelling under a constant volume condition, the stress point moves horizontally in the e-logp' plane with the increase in the degree of saturation, and it approaches the normal consolidation line (Sridharan et al. 1986). Furthermore, the equilibrium swelling pressure, namely the equilibrium vertical pressure at the initial void ratio, decreases when the specimen is confined insufficiently during saturation, in addition to the dry density dependency (Tanaka and Watanabe 2019). It is plausible that the equilibrium swelling pressure can contact the normal consolidation line if the compacted bentonite is sufficiently constrained and saturated. At each void ratio, the equilibrium swelling pressure and vertical confining pressure were balanced, which resulted in the stress path of the specimen without consolidation upon unloading along the normal consolidation line. This is presumably owing to the swelling deformation for maximum work efficiency. Meanwhile, it is presumed that the stress path upon unloading diverge from the normal consolidation line when the efficiency of swelling deformation was reduced.

This study focused on the fact that the effective stress in the radial direction became larger than that in the axial direction along unloading. This experimental fact indicates the anisotropy of the swelling pressure. It has been reported that the anisotropy of swelling pressure occurs when dry density of compacted bentonite is low (Saba et al. 2014); thus, considering the montmorillonite content, the interpretation in this study seems to be consistent. As shown in Figure 4, the ratio σ'_r/σ'_a changed

continuously upon unloading, which was different from that in the normal consolidation process. By causing even the slightest deformation to the specimen, the effective stress in the radial direction increased while that in the axial direction decreased. This is probably a reason why the equilibrium swelling pressure decreases when the specimen confinement is insufficient. Further unloading showed one-dimensional swelling deformation and $\sigma'_r \geqq \sigma'_a$. Therefore, in this phenomenon, it can be interpreted that the plastic swelling deformation satisfied the Mohr–Coulomb failure criteria (Eq. 1).

$$\sigma'_r/\sigma'_a = (1+\sin\emptyset')/(1-\sin\emptyset') \quad (1)$$

The result of the consolidation-undrained triaxial compression test of Kunigel-V1 (Namikawa et al. 2004) is shown in Figure. 6. The deviator stress maintained a constant value, which was almost the same as the peak in the range of more than 4% of the axial strain. The internal friction angle, ϕ', was 16.5°. Assuming this is in the critical state, i.e. an axial strain of more than 4% corresponds to a shear strain of more than 6%, then in the range of swelling rate of more than 6%, it can be calculated using Eq. 1 that σ'_r is approximately 1.8 times of σ'_a. Conversely, for the condition of $\sigma'_r < \sigma'_a$, σ'_r is approximately 0.56 times of σ'_a, which is harmonic with the results depicted in Figure 4.

As an interpretation of nonlinearity of swelling line, the discussion above is schematically illustrated in Figure 7. Owing to the anisotropy of swelling pressure, it is presumed that the effective stress in the axial direction, namely the vertical swelling pressure, decreased by unloading, and balanced between the constrained and swelling pressures; thus, resulting in a smaller swelling rate. Further unloading decreases the effective stress in the axial direction, and increases σ'_r/σ'_a. Therefore, it is expected that the osmotic swelling suppressed in the earlier unloading stage is more likely to occur with a higher mean effective stress.

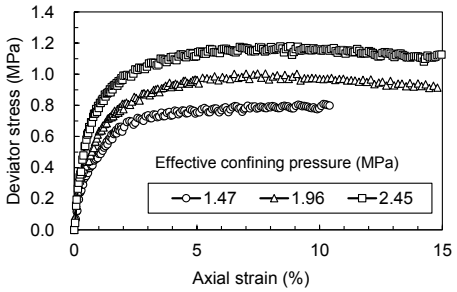

Figure 6. Result of consolidation-undrained triaxial compression test of Kunigel-V1, 1.6 Mg/m^3 of dry density (Namikawa et al. 2004).

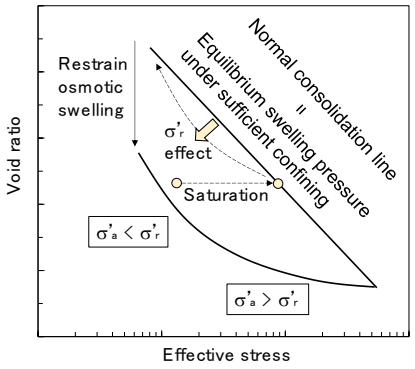

Figure 7. An interpretation of nonlinearity of swelling line in terms of the change in effective stress in axial direction by unloading.

5 CONCLUSIONS

This study performed a one-dimensional consolidation-swelling test using compacted Na-bentonite. Furthermore, a one-dimensional swelling deformation test using that without a consolidation history after saturation was performed. Unloading changed the effective stresses in the axial and radial directions, which caused the anisotropy of the effective stress upon unloading. Moreover, the nonlinearity of the swelling line on the *e*-log*p*' plane became smaller when using the compacted Na-bentonite without a consolidation history after the equilibrium swelling pressure was measured under a constrained condition. This study demonstrated an interpretation of the nonlinearity in terms of the change in the effective stress in the axial and radial directions upon unloading.

REFERENCES

Chapman, N. and Hooper, A. 2012. The disposal of radioactive wastes underground, *Proceedings of the Geologists' Association*, 123, 46–63.

Chen, Z.-G., Tang, C.-S., Zhu, C., Shi, B. and Liu, Y.-M. 2017. Compression, swelling and rebound behavior of GMZ bentonite/additive mixture under coupled hydro-mechanical condition, *Engineering Geology*, 221, 50–60.

Guerra, A. M., Cui, Y-J., He, Y., Delage, P., Mokni, N., Tang, A. M., Aimedieu, P., Bornert, M. and Bernier, F. 2019. Characterization of water retention, compressibility and swelling properties of a pellet/powder bentonite mixture, *Engineering Geology*, 248, 14–21.

Guimarães, L. D. N., Gens, A., Sánchez, M. and Olivella, S. 2013. A chemico-mechanical constitutive model accounting for cation exchange in expansive clays, *Géotechnique*, 63, No. 3, 221–234.

Komine, H. and Ogata, N. 1999. Experimental study on swelling characteristics of sand-bentonite mixture for nuclear waste disposal, *Soils and Foundations*, 39, No. 2, 83–97.

Komine, H. 2019. Scale-model test for disposal pit of high-level radioactive waste and theoretical evaluation on self-sealing of bentonite-based buffers, *Canadian Geotechnical Journal*, https://doi.org/10.1139/cgj-2018-0805.

Kyokawa, H., Ohno, S. and Kobayashi, I. 2020. A method for extending a general constitutive model to consider the electro-chemo-mechanical phenomena of mineral crystals in expansive soils, *International Journal for Numerical and Analytical Methods in Geomechanics*, 1–23.

Namikawa, T., Hirai, T., Tanai, K., Yui, M., Shigeno, Y., Takaji, K. and Ohnuma, M. 2004. Study on applicability of elasto-viscoplastic models to mechanical properties of compacted bentonite, *Journal of Japan Society of Civil Engineering*, No.764, III-67, 367–372. (in Japanese)

Saba, S., Barnichon, J.-D., Yu-Jun Cui, Y.-J., Anh Minh Tang, A. M. and Delage, P. 2014. Microstructure and anisotropic swelling behaviour of compacted bentonite/sand mixture, *Journal of Rock Mechanics and Geotechnical Engineering*, 6, 126–132.

Sahara, F., Murakami, T., Kobayashi, I., Mihara, M. and Ohi, T. 2008. Modelling for the long-term mechanical and hydraulic behavior of bentonite- and cement-based materials considering chemical transitions, *Physics and Chemistry of the Earth*, 33, S531-S537.

Sellin P. and Olivier, X. L. 2012. The use of clay as an engineered barrier in radioactive-waste management -a review, *Clays and Clay Minerals*, 61, No. 6, 477–498.

Sridharan, A., Rao, A. S. and Sivapullaiah, P. V. 1986. Swelling pressure of clays, *Geotechnical Testing Journal*, 9, No. 1, 24–33.

Takayama, Y., Tachibana, S., Iizuka, A., Kawai, K. and Kobayashi, I. 2017. Constitutive modeling for compacted bentonite buffer materials as unsaturated and saturated porous media, *Soils and Foundations*, 57, 80–91.

Tanaka, Y. and Nakamura, K. 2005. Effect of seawater and high-temperature history on swelling characteristics of bentonite, *Journal of Japan Society of Civil Engineering*, 806, III-73, 93–111. (in

Japanese)
Tanaka, Y. and Watanabe, Y. 2019. Modelling the effects of test conditions on the measured swelling pressure of compacted bentonite, *Soils and Foundations*, 59, 136–150.
Wang, Q., Tang, A. M., Cui, Y., Delage, P., Barnichon, J. and Ye, W. 2013. The effects of technological voids on the hydro-mechanical behavior of compacted bentonite–sand mixture, *Soils and Foundations*, 53, No. 2, 232–245.
Watanabe, Y. and Yokoyama, S. 2020. Montmorillonite content of bentonites considering accuracy of methylene blue adsorption test, *Journal of Japan Society of Civil Engineering*, 76, No.1, 26–39. (in Japanese)
Watanabe, Y. and Yokoyama, S. 2021. Self-sealing behavior of compacted bentonite-sand mixtures containing technological voids, *Geomechanics for Energy and the Environment*, 25, 100213, https://doi.org/10.1016/j.gete.2020.100213.
Zhang, C. and Kröhn, K. 2019. Sealing behavior of crushed claystone–bentonite mixtures, *Geomechanics for Energy and the Environment*, 17, 90–105.